Journal of Applied Physics PERSPECTIVE scitation.org/journal/jap

Electrical spectroscopy methods for the characterization of defects in thin-film compound solar cells

Cite as: J. Appl. Phys. **131**, 240901 (2022); doi: 10.1063/5.0085963
Submitted: 20 January 2022 · Accepted: 5 June 2022 ·
Published Online: 27 June 2022

View Online Export Citation CrossMark

M. Igalson[a] and A. Czudek

AFFILIATIONS

Faculty of Physics, Warsaw University of Technology, Koszykowa 75, 00-662 Warszawa, Poland

[a]**Author to whom correspondence should be addressed:** malgorzata.igalson@pw.edu.pl

ABSTRACT

The electronic activity of defects and their impact on the efficiency of Cu(In,Ga)Se_2 and CdTe solar cells is a subject of continuing interest and dispute in the photovoltaic community. However, after many years of research, the conclusions are far from satisfying yet. Here, the electrical defect spectroscopy results for Cu(In,Ga)Se_2 and CdTe absorbers and devices are discussed with focus on findings that have been confirmed on many samples but still do not have a well-grounded interpretation. Charged grain boundaries are proposed as a possible source of some signatures observed in deep level spectra in both materials. Electrical nano-characterization methods combined with standard defect spectroscopy are suggested as a promising solution for unraveling the role and origin of dominating defects for solar cells efficiency.

I. INTRODUCTION

Although deep defects in the absorbers of thin film solar cells can significantly reduce their efficiency, their influence and origin are not yet fully understood. This holds especially true for compound semiconductor-based cells. The development of sophisticated imaging methods, showing the structure and morphology of the devices on the atomic scale, sometimes makes electrical measurements look outdated. However, interpretations based solely on those methods do not illustrate the electrical activity of the observed features and may lead to conclusions that are not entirely justified. In this contribution, after a short overview of the electrical defect spectroscopy methods, we will discuss the literature data on defects in Cu(In,Ga)Se_2 (CIGS) and CdTe absorbers. Our aim is to present a comprehensive picture of deep levels, highlight interpretational ambiguities, and identify the common characteristics in the often chaotic picture of deep defect levels found by electrical spectroscopy. Arguments are presented for considering positively charged grain boundaries as a possible source of signals observed by capacitive spectroscopy. Finally, we will examine possibilities created by new methods of nanoscale characterization.

II. METHODS

Most electrical defect spectroscopy methods are based on the detection of thermal emission from trap levels e_T, which depends on the trap depth E_T and the capture cross section for emitted carriers σ_e,

$$e_T = \nu_0 \exp\left(-\frac{E_T}{k_B T}\right) = N_{C,V} \nu_{th} \sigma_{e,h} \exp\left(\frac{-E_T}{k_B T}\right). \quad (1)$$

In case of a point defect, a pre-exponential factor ν_0 depends on $\sigma_{e,h}$, on $N_{C,V}$—the density of states in the appropriate band, and on ν_{th}—the thermal velocity of an electron or a hole. An Arrhenius plot of the emission rates derived from the experiment provides the values of electrical parameters of the traps, and in the ideal case, it is a unique signature of a given defect level.

Popular methods of defect spectroscopy might be divided into two groups: steady-state methods based on the ac modulation of the equilibrium occupation of deep defect levels, such as admittance spectroscopy (AS) or modulated photocurrent spectroscopy (MPC), and transient methods in which a voltage and/or light pulse modifies the occupation of the defect and subsequent relaxation to the equilibrium state is observed [deep level transient spectroscopy (DLTS), deep level optical spectroscopy (DLOS) or transient photocapacitance spectroscopy (TPC), and photoinduced current transient spectroscopy (PICTS)]. Another classification is between methods based on measuring capacitance of the junction

(solar cell or Schottky) and on the investigation of (photo) conductivity of thin films. The capacitance methods are discussed extensively by Blood and Orton.[1] Information on how to determine the density of the trap levels, their spatial distribution, etc., can also be found there. Explanations on MPC and PICTS are presented in the original publications,[2–4] while TPC is explained in Ref. 5.

AS is the most popular method of defect spectroscopy as it is easy to implement and not demanding regarding junction quality. A favored method of presenting the admittance spectra as a density of states $N_T(E)$ was developed by Walter *et al.*[6] In this method, the admittance spectra are recalculated into the densities of trap states, which are then plotted as a function of energy instead of ac frequency by using a reverted relationship (1). This way of presentation has two significant flows. First, such a plot gives the impression of a continuous distribution of defect levels even when the level is, in fact, discrete. More importantly, information on the capture cross section for a given peak is not readily available to the readers—in many publications, only the density of states plot is reported. Comparisons between literature data based on just one parameter—activation energy—are not entirely reliable. In our opinion, only the analysis and comparison of the Arrhenius plots allow the identification and grouping of the signatures belonging to the same defect.

Methods based on photocurrent measurements such as MPC and PICTS applied to thin films have one advantage over capacitive ones—their sensitivity solely to the bulk levels in the absorber without distortions caused by the interfaces. Their major drawback is that under illumination by supra-bandgap photons concurring recombination processes might make detecting of the deep levels, especially these dangerous ones acting as the recombination centers, impossible. Thus, photocurrent methods are perhaps not reliable tools for detecting defect levels but are a valuable complementary method, helping us to distinguish bulk levels in the absorber from signatures originating from the front or back interface.

III. OVERVIEW OF THE DEFECT SPECTRA

A. CIGS absorbers and devices

Multiple reports on defect levels in photovoltaic materials and structures observed by capacitance and photocurrent spectroscopy have been published over the years. The results for CIGS devices can be summarized as follows: several electron and hole traps were found, but their origin and importance for solar cell efficiency is still not clear. The assignment of trap signatures to specific defects appears to be complicated because of a considerable variation in the apparent defect parameters, their dependence on the history, and treatments of the samples.

Above 250 K, the processes due to the creation and relaxation of the phenomenon typical for CIGS—metastabilities due to illumination and/or voltage pulses—result in the pronounced capacitance or conductivity transients. According to the Lany–Zunger model,[7] these transients correspond to a change of the configuration of a V_{Se}–V_{Cu} divacancy and, in fact, do not correspond to deep levels in the energy gap. In particular, the temperature dependence of the relaxation process is related to the potential barrier between two configurational states. The relaxation stretches over many orders of time and distorts all kinetics, which might be observed by transient methods at temperatures close to room temperature.[8] That effect complicates the analysis of the results on deep levels revealed at high temperatures by electrical defect spectroscopy.

The impression of chaos in that area is enhanced by the scarcity of systematic studies on single crystal samples that could be used as a reference as well as not careful enough analyses of the data. In our discussion below, we will focus on signatures observed in many samples, some of them studied from the beginning of research by electrical spectroscopy but not explained in a satisfactory manner. Our aim will be to find common points and eventually propose a more unified picture.

1. "N1" level

The so-called N1 level is observed in most devices and, together with another commonly met N2 level, was reported in the earliest papers on the capacitance spectroscopy in CIGS cells[10] and under various symbols in many other papers since then.[9,11–20] Typical DLTS spectrum of N1 and N2 traps is shown in Fig. 1 (after Ref. 9). The N1 level, a minority carrier trap, is the most common signature observed in nearly all devices, including Schottky diodes. It is a prominent feature in both DLTS and admittance spectra, detected at temperatures below 200 K and exhibiting varying activation energy of 50–200 meV. The sign of the DLTS signal indicating a minority carrier trap is its peculiar trait since no injection of minority carriers is required. Another unusual feature is its varying activation energy not only between samples, being generally lower in samples with higher hole density,[21,22] but also depending on the metastable state of the sample. A metastable decrease of the activation energy after light soaking[23] is typically observed and makes standard interpretation as a point defect signature dubious. Interestingly, a Meyer–Neldel rule relates its activation energy E_T to the pre-exponential factor ν_0, especially in the

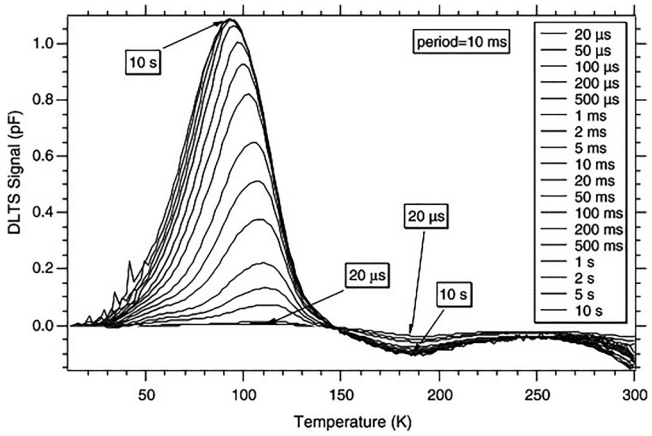

FIG. 1. DLTS spectrum showing the peaks corresponding to the N1 minority (positive peak at low temperature) and N2 majority carrier trap (negative signal around 180 K) (after AbuShama *et al.*[9]). Reproduced with permission from AbuShama *et al.*, J. Phys. Chem. Solids **66**, 1855 (2005). Copyright 2005 Elsevier Ltd.

case of illumination-induced changes of E_T and ν_0.[24–26] One more characteristic property of the N1 level is a logarithmic dependence of the magnitude of DLTS response on the length of the voltage pulse extending for many orders of magnitude of time [see Fig. 1 (Ref. 9) and Ref. 21]. This feature alone indicates extended defects as its origin.

A source of the N1 signature was most frequently discussed, and various models were proposed. It was attributed, e.g., to the front interface states[10,27,28] or Schottky contact at the back electrode.[29–31] However, none of these models were able to explain all its specific features, especially varying activation energy and pre-exponential factor after light soaking. The front and back interface-related interpretations were also put in question by the results of photocurrent spectroscopy: signatures exhibiting similar emission rates as the N1 signal in CIGS cells and similarly depending on light soaking were observed also in thin films prepared in the same process as absorbers in corresponding devices. It is a strong argument that N1 originates in the bulk CIGS.[17,32]

A coherent interpretation of all observations regarding the N1 signature might be proposed basing on recent research on the electrical activity of grain boundaries. The calculations done by Lauwaert *et al.*[31] showed that the DLTS spectrum and its specific features, including the sign (indicating a minority carrier trap), might be reproduced within the model of a secondary barrier in the back of the device. Then, Wiśniewski *et al.*[33] proposed that potential barriers belonging to charged grain boundaries might result in such a DLTS spectrum. Sozzi *et al.*[34] found that the admittance spectra calculated within a model of defects at the front interface feature a much lower step height than observed experimentally, while the assumption of back contact barrier or charged grain boundary gives results closer to the experiment.

All these calculations show that the hypothesis of a secondary barrier, be it a back diode or a potential barrier at the grain boundary, should not be dismissed as the explanation of the N1 signature. What is even more important is that several experimental findings also indicate that the charged grain boundaries heavily influence electrical characteristics. A detailed investigation by AS, which included the determination of resistivity and carrier mobility in the absorber, provided strong support for the hypothesis of grain boundary (GB) barriers being responsible for the N1 peak and temperature dependence of mobility.[35] The findings on the impact of sodium and potassium on the electrical properties of thin films and solar cells doped with varying amounts of alkalis offered further evidence on the role of GB's in electrical transport and their passivation by alkali elements.[36,37] An analysis of the capacitance profiling data and the resistivity of thin films containing various amounts of sodium and potassium introduced by post-deposition treatment led to the conclusion that the effective mobility in the planar samples is limited by alkali-dependent potential barriers at the grain boundaries. This approach also explains a dependence of free hole density derived from capacitance profiling on the concentration of light alkali metals.[38] Furthermore, a correlation between the activation energy of the N1 level appearing in the defect spectra of solar cells and activation energy of conductivity in planar thin films was found.[21] That correlation points to the same source responsible for the barriers limiting the mobility of free carriers and for the activation energy of the admittance signal. Light-soaking effects together with the Meyer–Neldel relationship between activation energy of N1 signature and its pre-exponential factor ν_0 within this model reflect the illumination-induced change in the amount of positively charged donor-type defects responsible for the potential barriers. Even the correlation between the activation energy of the N1 signature and the barrier height derived from the current–voltage characteristics at far forward bias observed in Refs. 27 and 39 found a simple explanation since both reflect the same property of polycrystalline CIGS: the transport limited by potential barriers due to charged defects at GB. While a proposed explanation of the N1 signal as due to GBs limited transport is presently only a hypothesis requiring more research to be confirmed, we believe that an accumulating number of experimental facts makes it a plausible one and not to be neglected in further studies.

2. "N2" level

In Fig. 2, an example of the energetic distribution of trap density showing both N1 and N2 levels derived from admittance by using the method of Walter *et al.*[6] is presented (after Hanna *et al.*[40]).

In contrast to the N1 level, the N2 signal exhibits a fairly consistent signature, with thermal activation energy close to 0.3 eV in most reports, which included Schottky junctions;[16,18,27,41] thus, its assignment to the bulk defect level is not controversial. The saturation of the DLTS signal height is achieved already at a much shorter pulse length (see Fig. 1, Ref. 9). Its apparent concentration, as derived from the AS measurements, depends on a variety of factors. Already in the first study of the DLTS spectrum and metastabilities, it was shown that heavy injection produces an increase of N2 density.[42] In most reports published during the following decades, the N2 level was rarely found in high-efficiency devices. However, analysis of the literature data provides puzzling information on the correlations between a device efficiency loss due to various treatments and the concentration of the N2 defect. It was found to be correlated with the gallium content and device

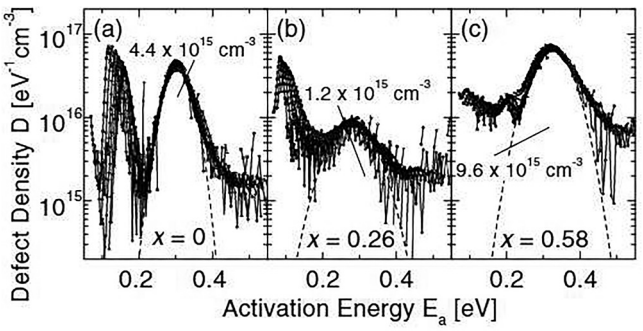

FIG. 2. The trap states density derived from admittance measurements in CIGS devices with various gallium contents x = Ga/(In + Ga): (a) x = 0; (b) x = 0.26; and (c) x = 0.58 (after Hanna *et al.*[40]). The activation energy of N1 peak is about 0.1 eV and of N2 peak is equal to 0.3 eV. Reproduced with permission from Hanna *et al.*, Thin Solid Films **387**, 71 (2001). Copyright 2001 Elsevier Science B.V.

efficiency—one example is presented in Fig. 2.[40,41] Similar correlation between efficiency and increased concentration of the level at 0.3 eV was then found in many samples: in the series of cells with increasing selenium deficiency during growth,[11] doped with Ni,[13] after electron or proton irradiation,[43] and also after "damp heat" treatment (prolonged heating at elevated temperature in the humid atmosphere).[19] Alkali metals supplied during or after growth of the CIGS layer also affect both the performance of the CIGS cells and the N2 signal. No sodium results in samples with prominent N2 signature and low efficiency; in samples containing sodium, the efficiency was enhanced and the N2 signal was reduced or not observed at all.[25,36,44] The more so fabrication procedure that included potassium doping during growth resulted in samples with prominent N2 peak and lower efficiency, while potassium fluoride KF post-deposition treatment reduced N2 peak and increased doping and efficiency.[45] The puzzling issue is that those very different treatments led to similar results: correlation of the (apparent) N2 concentration and the device efficiency. It is hard to believe that these very different procedures mentioned above enhanced the concentration of one defect. In our opinion, all these results evidently show that the magnitude of the N2 signature reflects the presence of some deficiency in the cell, but it is not necessarily related to the concentration of the N2 defect itself. It rather documents that efficiency loss and a presence of the prominent N2 signal goes beyond simple interpretation of the enhanced point defect concentration.

3. Midgap and above midgap levels

Very deep levels due to their low emission rates at temperatures below 300 K are not accessible by the most popular steady-state method—admittance spectroscopy. Their presence might be documented only by transient methods, DLTS, DLOS, TPC, or PICTS, at room temperature or above. In this temperature range, both voltage and light pulses might produce large capacitance or conductivity transient due to metastable defect conversion, as explained earlier. We believe that these effects contribute to the variation of the parameters derived from DLTS or DLOS measurements performed at high temperatures such as reported, e.g., in Refs. 46 and 47.

One of the deep levels that were observed on a couple of samples in various laboratories by DLTS and DLOS close to the room temperature is a deep trap of activation energy around 0.50 eV.[48–51] It was also found by PICTS in both polycrystalline[52] and epitaxial layers.[53] This is strong evidence that the level belongs to the bulk of the absorber. As reported in many papers, although it was revealed at the same temperature range, a considerable variation of the activation energies was observed (0.46–0.61 eV). While accompanying metastabilities might be held responsible, other explanations such as the defect's location in various environments are possible. That defect indeed was identified by scanning DLTS at grain boundaries,[15] which makes such an explanation plausible.

TPC measurements by Heath *et al.* revealed one more very deep level of energy 0.8 eV above the valence band by using a combination of voltage and monochromatic light pulses.[5] No assignment to any of the intrinsic point defects was proposed up to date. However, one might notice that the properties of the DX state of III_{Cu} defect predicted in Ref. 54 agree with this level very well and substantiate the thesis that it might be responsible for the performance losses of high gallium absorbers. Interestingly, a deep radiative recombination state around 0.7–0.8 eV was observed in the photoluminescence spectrum of CIGS and $CuGaSe_2$ epitaxial layers. It was attributed though to the Cu_{III} antisite, which is less probable in the In-rich polycrystalline CIGS composition.[55]

An even deeper level, around 0.98–0.99 eV above the valence band, was found by several researchers by using the DLOS method.[48–51] Since these observations are made in the high temperature region and by methods involving optical excitation, the V_{Se}–V_{Cu} divacancy might indeed be the origin of this signal as proposed by Ferguson *et al.*[50] In our opinion, a plausible assignment would be an antisymmetric level of the divacancy in the acceptor configuration; however, more experiments should confirm that this level appears only in the acceptor (metastable) state of the defect.

B. CdTe-based devices

Defect spectroscopy applied to CdS/CdTe solar cells also brought results that do not provide definitive answers. Although data for single crystal CdTe, which can be used as reference, can be found in abundance in the literature,[56] the results of AS and DLTS measurements bring many controversies. While numerous defect levels were found and assigned to various intrinsic defects, which might be expected in CdTe, these assignments were rather speculative, rarely based on thorough discussion.[57–63] In particular, several relatively shallow levels with activation energy below 0.2 eV were designated as various point defects in CdTe. However, the low doping of absorbers under study indicates that the Fermi-level is situated at least at 0.24 eV above the valence band, so observing that shallow majority carrier traps is not possible. Some of the signatures revealed by DLTS exhibit a positive DLTS sign, which identifies them as electron traps. The example is shown in Fig. 3 (after Ref. 63). This feature is similar to the observations made in CIGS—a signal due to minority carriers observed without minority carrier injection. Again, as in the CIGSe devices, there are also opinions that some of the apparent defect levels found in CdTe cells do not correspond to the point defects: the shallow ones with energies lower than 150 meV reflect the height of the potential barriers at the grain boundaries and the deeper—to the back contact barrier (Ea around 0.2–0.3 up to 0.45 eV).[61] A convincing analysis of the admittance spectrum featuring the signal due to the back contact barrier and depending on the annealing temperature was presented by Paul *et al.*[62] They also proposed that the signatures around 80–150 meV were related to the potential barriers at GBs. We would like to note here the interesting similarity between the DLTS spectra of the CdTe device reported by Ding *et al.*[63] (Fig. 3) and DLTS spectrum of the N1 and N2 levels in CIGS shown in Fig. 1. Particularly, a dependence of the minority signal on pulse length indicates that the signal originates from extended defects. While it might be pure coincidence, one cannot exclude that both N1 and N2 levels and these two levels in CdTe are a manifestation of the same effect, somehow related to the grain boundaries.

We conclude that similarly as in the case of CIGS, a picture of dominating defect levels in CdTe absorbers, their dependence on technological procedures, and their impact on efficiency is far from

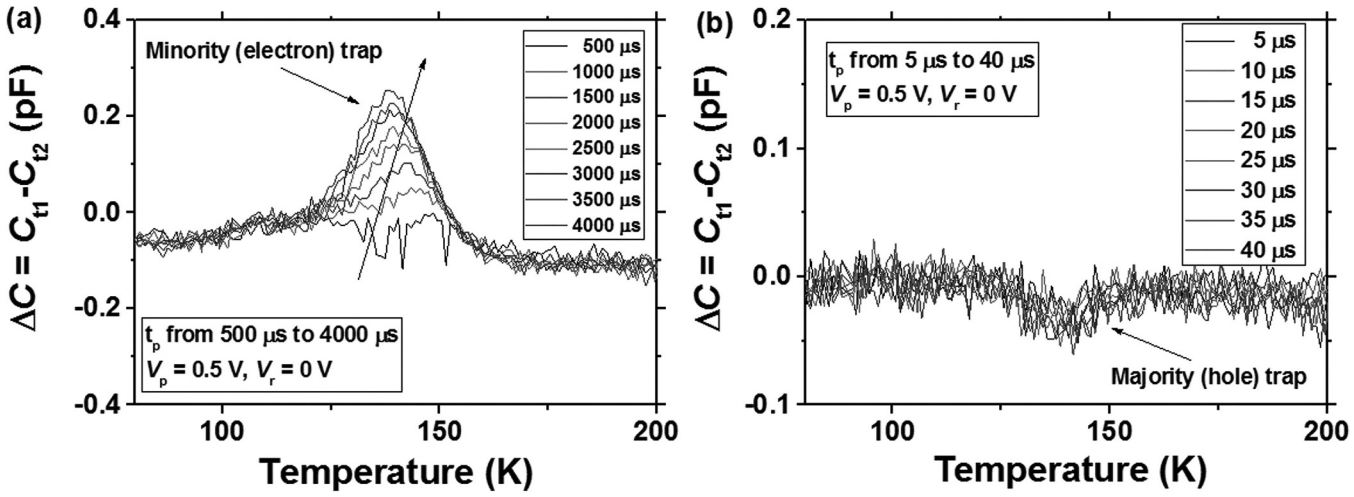

FIG. 3. DLTS spectra observed in CdTe solar cell measured at 866 s^{-1} emission window for increasing pulse length t_p: (a) long pulses from 500 to 4000 μs and (b) short pulses from 5 to 40 μs (after Ding *et al.*[63]). Reproduced with permission from Ding *et al.*, J. Appl. Phys. **120**, 135704 (2016). Copyright 2016 AIP Publishing LLC.

clear yet. However, more and more evidence point toward other than point defects origin of some of the observed signatures. In particular, the contribution of secondary barriers, such as due to grain boundaries and interfaces to the signals observed by electrical spectroscopy methods, requires more research.

IV. CONCLUSIONS AND PERSPECTIVES

Looking through the literature, one can get the impression that electrical defect spectroscopy in compound photovoltaic materials brings more questions than answers. Partly, it is a result of the superficial character of many studies, which offer an explanation for one aspect of the experimental results but overlook other aspects. The issue neglected so far is the influence of charged grain boundaries on the electrical characteristics. First, as shown by Urbaniak *et al.*,[38] the potential barriers at GB's in CIGS might distort the measured capacitance value. Hence, free hole concentrations and depletion widths derived from capacitance measurements are also distorted, and this has to be taken into account in all evaluations, in particular, concerning trap density. Thus, the apparent N2 level concentration changes correlated with the device efficiency might be a by-product of changing properties of the grains, i.e., their passivation, or to the contrary, the damage induced by, e.g., electron bombardment, "damp heat" treatment, or too low selenium pressure. Whether the N2 signature belongs also to a defect at the grain boundaries or to the one of dominating defects in the bulk of the grains, which response is modified by the grain barriers, requires further studies. The importance of this research from the point of view of identifying the main factors having an impact on the efficiency of solar cells is considerable, and the correlation between high N2 concentration and efficiency has been confirmed many times over the last 20 years.

The N1 signal in our opinion seems to be directly related to the GB barriers. This hypothesis is supported by simulations and by many experimental findings. Among them are results on sodium- or potassium-treated devices and thin films,[36,37] the detailed analysis of the admittance, capacitance–voltage, and resistivity of the solar cells in Ref. 35. Furthermore, the recent work of Tangara *et al.*[64] showed that Rb treatment of absorbers reduces the activation energy of the N1 peak. However, this hypothesis requires more experimental evidence and 2D simulations. If proven, then the parameters of the N1 signature could provide information on the height of the potential barriers and the concentration of defects at GBs. Thus, we could get an indispensable tool guiding the efforts to optimize the treatments leading to the passivation of grain boundaries. The same goes for the CdTe solar cells. Here, the identification by defect spectroscopy of the signatures originating from the secondary belonging to the grain boundaries also provides information on the state of GB's and the degree of their passivation by chemical treatments. The experimental evidence on the recombination activity of GBs is shown, e.g., in the work of Kanevce *et al.*,[65] and the quite surprising similarity of the DLTS spectra shown in Fig. 3 confirms that further investigations in this direction are needed.

More information on the input of GBs to the electrical characteristics of the photovoltaic devices might be brought by a combination of the traditional methods of electrical defect spectroscopy together with novel tools enabling us to look into the material properties in the nanoscale. They should allow us to assess not only microstructural and compositional properties of GB such as atom probe tomography investigation on the distribution of various elements including alkali metals at GBs reported in Ref. 66 but also show the relationship between composition and electrical activity of GBs. Good examples are investigations by a combined atom probe tomography APT, electron beam induced current (EBIC), and electron backscatter diffraction (EBSD)[67] or the assessment of

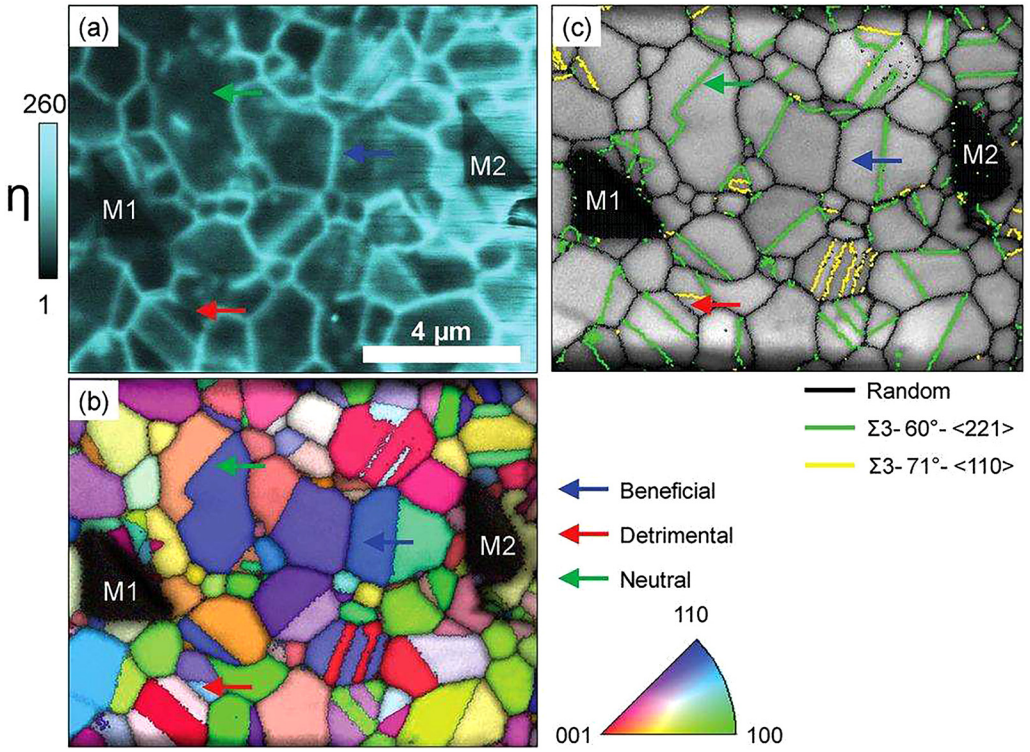

FIG. 4. Correlative EBIC–EBSD investigation revealing the position of benign, detrimental, and neutral GBs in the CIGS absorber. (a) Quantitative EBIC map represents the current collection, in which contrast (bright) is proportional to the EBIC current. (b) EBSD texture map represents the distribution of grains and location of GBs from the same region. (c) EBSD grain boundaries map revealing random (black), twin 60° (green), and twin 71° (yellow) boundaries (after Raghuwanshi *et al.*[67]). Reproduced with permission from Raghuwanshi *et al.*, Adv. Funct. Mater. **30**, 2001046 (2020). Copyright 2020 Wiley-VCH GmbH.

the electrostatic potential fluctuations and resulting space charge width fluctuations in the nanoscale by Krause *et al.*[68] However, the reports of Raghuwanshi *et al.*[67,69] show how complicated is the issue of recombination activity at the grain boundaries. They found that the benign or detrimental character of the GBs depends on their type and composition. The results are depicted in Fig. 4.

A study of correlation between electrical properties by electron beam currents and composition by APT in the nanoscale was also performed in CdS/CdTe solar cells.[70] It was found that Cu and Cl at GB mitigated the recombination activity of the GB, while Na had no effect.

These correlative methods, albeit they provide insight into the properties of grain boundaries, do not have a direct translation into photoelectric and capacitive characteristics of the devices under study yet. The exemption is the studies of Paul *et al.*[15] and Deitz *et al.*[71] In the work of Paul *et al.*, the surface potential transients were correlated with the conventional DLTS signal corresponding to a 0.47 eV trap and attributed it to the GBs. In the work of Deitz *et al.*, electron energy loss spectroscopy, scanning electron transmission spectroscopy, and scanning DLTS also identified traps close to midgap in the grain boundary region. These defects as positively charged donors might be responsible for potential barriers at grain boundaries. We see the continuation of work in this direction as one of the future paths for extending our knowledge on defects activity in the absorbers of thin film solar cells and their accumulation at specific structures.

V. SUMMARY

The data published over the last two decades on defect signatures detected by the electrical spectroscopy in the case of CIGS allowed us to distinguish five major groups of levels (the energies are given relatively to the valence band):

- N1 level, $E_T = 50–240$ meV: attributed in the literature to the front interface response or to back diode, but in our opinion, it might be directly related to the potential barriers at the grain boundaries.
- N2 level, $E_T = 300–320$ meV: point defect of apparent concentration correlated to the efficiency of solar cells. The reason for that correlation is not well understood. We propose that those concentrations deduced from admittance spectroscopy might be distorted by the presence of internal barriers related to a degree of passivation of grain boundaries and other interfaces.
- Midgap levels close to 0.50 eV: the 0.47 eV signature is the only level directly observed at the grain boundary, as a donor-type defect. Thus, it might be a positively charged defect responsible

for the potential barriers at GB. To confirm this hypothesis, more research also on alkali-free absorbers is required. A variation of the activation energies might come from different environments of defects situated at the grain boundary.
- 0.8 eV level: possible assignment—relaxed DX state of the III_{Cu} antisite.
- 0.89 eV level: proposed assignment—antisymmetric level belonging to the V_{Cu}–V_{Se} divacancy in the acceptor configuration. Experiments showing its relation to the metastable state of the sample should help confirm this assignment.

In the case of CdTe absorbers, we conclude that the levels with activation energies between 50 and 150 meV and sometimes attributed to shallow point defects are rather due to the potential barriers at the grain boundaries. Deeper levels between 200 and 400 meV, especially those indicating minority carrier emission without minority injection, might belong to the back contact barrier. Including the DLTS sign and dependence on pulse duration in the discussion should help make better-grounded assignments.

The overview of the results of defect spectroscopy in both CIGS and CdTe showed that too often the fact that we deal with polycrystalline materials was neglected. We believe that a more rigorous approach to the analysis of the results of classical defect spectroscopy methods should be supplemented by the experiments employing novel techniques, which provide insight into the electrical properties of materials and devices in the nanoscale. Such an approach should bring at last the in-depth understanding of the defect-related phenomena in photovoltaic materials and devices and, thus, help establish better optimized technological processes. This concerns, in particular, the issue of grain boundaries, their contribution to the efficiency losses and the effect of their passivation by alkali treatments in case of CIGS, and $CdCl_2$/Cu treatment in the case of CdTe.

ACKNOWLEDGMENTS

This work was partially supported by the National Science Centre, Poland (Contract No. 2016/23/G/ST5/04268) within the Beethoven II program, AlkaCIGS project. The inspiring discussions with Aleksander Urbaniak and Pawel Zabierowski are greatly appreciated.

AUTHOR DECLARATIONS

Conflict of Interest

The authors have no conflicts to disclose.

Author Contributions

M. Igalson: Conceptualization (lead); Writing – original draft (lead); Writing – review & editing (lead). **A. Czudek:** Writing – review & editing (supporting).

DATA AVAILABILITY

Data sharing is not applicable to this article as no new data were created or analyzed in this study.

REFERENCES

[1]P. Blood and J. W. Orton, *The Electrical Characterization of Semiconductors: Majority Carriers and Electron States* (Academic Press, 1992).
[2]C. Longeaud, J. P. Kleider, P. Kaminski, R. Kozlowski, and M. Miczuga, J. Phys.: Condens. Matter **21**, 045801 (2009).
[3]J. P. Kleider, C. Longeaud, and M. E. Gueunier, Phys. Status Solidi C **1**, 1208 (2004).
[4]C. Hurtes, M. Boulou, A. Mitonneau, and D. Bois, Appl. Phys. Lett. **32**, 821 (1978).
[5]J. T. Heath, J. D. Cohen, W. N. Shafarman, D. X. Liao, and A. A. Rockett, Appl. Phys. Lett. **80**, 4540 (2002).
[6]T. Walter, R. Herberholz, C. Müller, and H. W. Schock, J. Appl. Phys. **80**, 4411 (1996).
[7]S. Lany and A. Zunger, J. Appl. Phys. **100**, 113725 (2006).
[8]A. Urbaniak and M. Igalson, J. Appl. Phys. **106**, 063720 (2009).
[9]J. A. M. AbuShama, S. Johnston, and R. Noufi, J. Phys. Chem. Solids **66**, 1855 (2005).
[10]R. Herberholz, M. Igalson, and H. W. Schock, J. Appl. Phys. **83**, 318 (1998).
[11]T. Sakurai, M. M. Islam, H. Uehigashi, S. Ishizuka, A. Yamada, K. Matsubara, S. Niki, and K. Akimoto, Sol. Energy Mater. Sol. Cells **95**, 227 (2011).
[12]I. Khatri and M. Sugiyama, Appl. Phys. Lett. **118**, 113901 (2021).
[13]F. Pianezzi, S. Nishiwaki, L. Kranz, C. M. Sutter-Fella, P. Reinhard, B. Bissig, H. Hagendorfer, S. Buecheler, and A. N. Tiwari, Prog. Photovoltaics Res. Appl. **23**, 892 (2015).
[14]A. Krysztopa, M. Igalson, L. Gütay, J. K. Larsen, and Y. Aida, Thin Solid Films **535**, 366 (2013).
[15]P. K. Paul, D. W. Cardwell, C. M. Jackson, K. Galiano, K. Aryal, J. P. Pelz, S. Marsillac, S. A. Ringel, T. J. Grassman, and A. R. Arehart, IEEE J. Photovoltaics **5**, 1482 (2015).
[16]A. Urbaniak, K. Macielak, M. Igalson, P. Szaniawski, and M. Edoff, J. Phys.: Condens. Matter **28**, 215801 (2016).
[17]J. Serhan, Z. Djebbour, D. Mencaraglia, F. Couzinié-Devy, N. Barreau, and J. Kessler, Thin Solid Films **519**, 7312 (2011).
[18]C. Deibel, V. Dyakonov, and J. Parisi, Appl. Phys. Lett. **82**, 3559 (2003).
[19]M. Igalson, M. Wimbor, and J. Wennerberg, Thin Solid Films **403–404**, 320 (2002).
[20]T. Eisenbarth, T. Unold, R. Caballero, C. A. Kaufmann, D. Abou-Ras, and H. W. Schock, Thin Solid Films **517**, 2244 (2009).
[21]A. Urbaniak, K. Macielak, N. Barreau, P. Szaniawski, and M. Edoff, J. Phys. Chem. Solids **134**, 58 (2019).
[22]S. J. Heise, V. Gerliz, M. S. Hammer, J. Ohland, J. Keller, and I. Hammer-Riedel, Sol. Energy Mater. Sol. Cells **163**, 270 (2017).
[23]M. Igalson, M. Bodegård, L. Stolt, and A. Jasenek, Thin Solid Films **431–432**, 153 (2003).
[24]R. Herberholz, T. Walter, C. Muller, T. M. Friedlmeier, H. W. Schock, M. Saad, M. C. Lux-Steiner, and V. Alberts, Appl. Phys. Lett. **69**, 2888 (1996).
[25]P. T. Erslev, W. N. Shafarman, and J. D. Cohen, Appl. Phys. Lett. **98**, 062105 (2011).
[26]A. Urbaniak, M. Igalson, A. Krysztopa, A. Chirilă, S. Buecheler, F. Pianezzi, and A. N. Tiwari, Thin Solid Films **535**, 314 (2013).
[27]M. Igalson, A. Urbaniak, and M. Edoff, Thin Solid Films **517**, 2153 (2009).
[28]F. Werner and S. Siebentritt, Phys. Rev. Appl. **9**, 54047 (2018).
[29]T. Eisenbarth, T. Unold, R. Caballero, C. A. Kaufmann, and H.-W. Schock, J. Appl. Phys. **107**, 034509 (2010).
[30]D. Muecke, T. Lavrenko, R. V. Lorbada, and T. Walter, in *2018 IEEE 7th World Conference on Photovoltaic Energy Conversion (A Joint Conference of 45th IEEE PVSC, 28th PVSEC, & 34th EU PVSEC)* (IEEE, 2018), pp. 1928–1931.
[31]J. Lauwaert, J. Lauwaert, L. Van Puyvelde, J. W. Thybaut, and H. Vrielinck, Appl. Phys. Lett. **104**, 053502 (2014).
[32]K. Macielak, M. Igalson, A. Urbaniak, P. Zabierowski, and N. Barreau, in *2015 IEEE 42nd Photovoltaic Special Conference* (IEEE, 2015), pp. 1–4.
[33]K. Wiśniewski and P. Zabierowski, Thin Solid Films **721**, 138540 (2021).

[34]G. Sozzi, S. Di Napoli, R. Menozzi, T. P. Weiss, S. Buecheler, and A. N. Tiwari, in *2018 IEEE 7th World Conference on Photovoltaic Energy Conversion (A Joint Conference of 45th IEEE PVSC, 28th PVSEC, & 34th EU PVSEC)* (IEEE, 2018), pp. 2515–2519.
[35]S. Paul, R. Lopez, I. L. Repins, and J. V. Li, J. Vac. Sci. Technol. B **36**, 022904 (2018).
[36]A. Czudek, A. Eslam, A. Urbaniak, P. Zabierowski, R. Wuerz, and M. Igalson, J. Appl. Phys. **128**, 173102 (2020).
[37]A. Czudek, A. Urbaniak, A. Eslam, R. Wuerz, and M. Igalson, Phys. Status Solidi RRL **16**, 2100459 (2022).
[38]A. Urbaniak, M. Igalson, F. Pianezzi, S. Bücheler, A. Chirilă, P. Reinhard, and A. N. Tiwari, Sol. Energy Mater. Sol. Cells **128**, 52 (2014).
[39]F. Werner, M. H. Wolter, S. Siebentritt, G. Sozzi, S. Di Napoli, R. Menozzi, P. Jackson, W. Witte, R. Carron, E. Avancini, T. P. Weiss, and S. Buecheler, Prog. Photovoltaics Res. Appl. **26**, 911 (2018).
[40]G. Hanna, A. Jasenek, U. Rau, and H. W. Schock, Thin Solid Films **387**, 71 (2001).
[41]T. Sakurai, N. Ishida, S. Ishizuka, K. Matsubara, K. Sakurai, A. Yamada, G. K. Paul, K. Akimoto, and S. Niki, Thin Solid Films **515**, 6208 (2007).
[42]M. Igalson and H. W. Schock, J. Appl. Phys. **80**, 5765 (1996).
[43]A. Jasenek and U. Rau, J. Appl. Phys. **90**, 650 (2001).
[44]X. He, J. Liu, Q. Ye, K. Luo, Y. Jiang, C. Liao, L. Ouyang, D. Zhuang, J. Mei, and W. Lau, J. Alloys Compd. **658**, 12 (2016).
[45]F. Pianezzi, P. Reinhard, A. Chirilă, S. Nishiwaki, B. Bissig, S. Buecheler, and A. N. Tiwari, J. Appl. Phys. **114**, 194508 (2013).
[46]R. L. Garris, S. Johnston, J. V. Li, H. L. Guthrey, K. Ramanathan, and L. M. Mansfield, Sol. Energy Mater. Sol. Cells **174**, 77 (2018).
[47]L. L. Kerr, S. S. Li, S. W. Johnston, T. J. Anderson, O. D. Crisalle, W. K. Kim, J. Abushama, and R. N. Noufi, Solid State Electron. **48**, 1579 (2004).
[48]S. Karki, P. K. Paul, G. Rajan, T. Ashrafee, K. Aryal, P. Pradhan, R. W. Collins, A. Rockett, T. J. Grassman, S. A. Ringel, A. R. Arehart, and S. Marsillac, IEEE J. Photovoltaics **7**, 665 (2017).
[49]S. Karki, P. Paul, G. Rajan, B. Belfore, D. Poudel, A. Rockett, E. Danilov, F. Castellano, A. R. Arehart, and S. Marsillac, IEEE J. Photovoltaics **9**, 313 (2019).
[50]A. J. Ferguson, R. Farshchi, P. K. Paul, P. Dippo, J. Bailey, D. Poplavskyy, A. Khanam, F. Tuomisto, A. R. Arehart, and D. Kuciauskas, J. Appl. Phys. **127**, 215702 (2020).
[51]P. K. Paul, K. Aryal, S. Marsillac, T. J. Grassman, S. A. Ringel, and A. R. Arehart, in *2016 IEEE 43rd Photovoltaic Special Conference* (IEEE, 2016), pp. 3641–3644.
[52]K. Macielak, M. Igalson, P. Zabierowski, N. Barreau, and L. Arzel, Thin Solid Films **582**, 383 (2015).
[53]A. Krysztopa, M. Igalson, J. K. Larsen, Y. Aida, L. Gütay, and S. Siebentritt, J. Phys. D: Appl. Phys. **45**, 335101 (2012).
[54]S. Lany and A. Zunger, Phys. Rev. Lett. **100**, 016401 (2008).
[55]C. Spindler, F. Babbe, M. H. Wolter, F. Ehré, K. Santhosh, P. Hilgert, F. Werner, and S. Siebentritt, Phys. Rev. Mater. **3**, 090302 (2019).
[56]X. Mathew, Sol. Energy Mater. Sol. Cells **76**, 225 (2003).
[57]J. Versluys, P. Clauws, P. Nollet, S. Degrave, and M. Burgelman, Thin Solid Films **451–452**, 434 (2004).
[58]A. Balcioglu, R. K. Ahrenkiel, and F. Hasoon, J. Appl. Phys. **88**, 7175 (2000).
[59]I. Rimmaudo, A. Salavei, and A. Romeo, Thin Solid Films **535**, 253 (2013).
[60]E. Artegiani, P. Punathil, V. Kumar, M. Bertoncello, M. Meneghini, A. Gasparotto, and A. Romeo, Solar Energy **227**, 8 (2021).
[61]J. V. Li, S. W. Johnston, X. Li, D. S. Albin, T. A. Gessert, and D. H. Levi, J. Appl. Phys. **108**, 064501 (2010).
[62]S. Paul, S. Sohal, C. Swartz, D.-B. Li, S. S. Bista, C. R. Grice, Y. Yan, M. Holtz, and J. V. Li, Solar Energy **211**, 938 (2020).
[63]Y. M. Ding, Z. Cheng, X. Tan, D. Misra, A. E. Delahoy, and K. K. Chin, J. Appl. Phys. **120**, 135704 (2016).
[64]H. Tangara, S. Zahedi-Azad, J. Not, J. Schick, A. Lafuente-Sampietro, M. M. Islam, R. Scheer, and T. Sakurai, J. Appl. Phys. **129**, 183108 (2021).
[65]A. Kanevce, J. Moseley, D. Kuciauskas, M. Al-Jassim, and W. K. Metzger, in *2015 IEEE 42nd Photovoltaic Special Conference* (IEEE, 2015), pp. 1–4.
[66]O. Cojocaru-Mirédin, M. Raghuwanshi, R. Wuerz, and S. Sadewasser, Adv. Funct. Mater. **31**, 2103119 (2021).
[67]M. Raghuwanshi, R. Wuerz, and O. Cojocaru-Mirédin, Adv. Funct. Mater. **30**, 2001046 (2020).
[68]M. Krause, A. Nikolaeva, M. Maiberg, P. Jackson, D. Hariskos, W. Witte, J. A. Márquez, S. Levcenko, T. Unold, R. Scheer, and D. Abou-Ras, Nat. Commun. **11**, 4189 (2020).
[69]M. Raghuwanshi, B. Thöner, P. Soni, M. Wuttig, R. Wuerz, and O. Cojocaru-Mirédin, ACS Appl. Mater. Interfaces **10**, 14759 (2018).
[70]J. D. Poplawsky, C. Li, N. R. Paudel, W. Guo, Y. Yan, and S. J. Pennycook, Sol. Energy Mater. Sol. Cells **150**, 95 (2016).
[71]J. I. Deitz, P. K. Paul, S. Karki, S. X. Marsillac, A. R. Arehart, T. J. Grassman, and D. W. McComb, in *2018 IEEE 7th World Conference on Photovoltaic Energy Conversion (A Joint Conference of 45th IEEE PVSC, 28th PVSEC, & 34th EU PVSEC)* (IEEE, 2018), pp. 3914–3917.